

MICROCOPY RESOLUTION TEST CHART
NATIONAL BUREAU OF STANDARDS 1963-A

DTIC FILE COPY

12



RADC-TR-86-101
Final Technical Report
November 1986

AD-A179 829

SUPERLUMINESCENT LED STUDY

GTE Laboratories Incorporated

Robert Olshansky

DTIC
S
MAY 01 1987
D
Y

APPROVED FOR PUBLIC RELEASE; DISTRIBUTION UNLIMITED

ROME AIR DEVELOPMENT CENTER
Air Force Systems Command
Griffiss Air Force Base, NY 13441-5700

87 4 30 087

This report has been reviewed by the RADC Public Affairs Office (PA) and is releasable to the National Technical Information Service (NTIS). At NITS it will be releasable to the general public, including foreign nations.

RADC-TR-86-101 has been reviewed and is approved for publication.

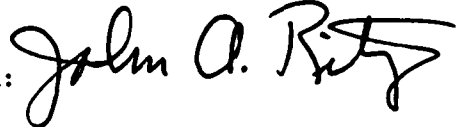
APPROVED:


JOSEPH P. LORENZO
Project Engineer

APPROVED:


HAROLD ROTH
Director of Solid State Sciences

FOR THE COMMANDER:


JOHN A. RITZ
Directorate of Plans & Programs

If your address has changed or if you wish to be removed from the RADC mailing list, or if the addressee is no longer employed by your organization, please notify RADC (ESO) Hanscom AFB MA 01731-5000. This will assist us in maintaining a current mailing list.

Do not return copies of this report unless contractual obligations or notices on a specific document requires that it be returned.

UNCLASSIFIED

SECURITY CLASSIFICATION OF THIS PAGE

AD-A179829

REPORT DOCUMENTATION PAGE

1a REPORT SECURITY CLASSIFICATION UNCLASSIFIED			1b RESTRICTIVE MARKINGS N/A		
2a SECURITY CLASSIFICATION AUTHORITY N/A			3 DISTRIBUTION / AVAILABILITY OF REPORT Approved for public release; distribution unlimited		
2b DECLASSIFICATION / DOWNGRADING SCHEDULE N/A					
4 PERFORMING ORGANIZATION REPORT NUMBER(S) N/A			5 MONITORING ORGANIZATION REPORT NUMBER(S) RADC-TR-86-101		
6a. NAME OF PERFORMING ORGANIZATION GTE Laboratories Incorporated		6b OFFICE SYMBOL (if applicable)	7a. NAME OF MONITORING ORGANIZATION Rome Air Development Center (ESO)		
6c. ADDRESS (City, State, and ZIP Code) 40 Sylvan Road Waltham MA 02254			7b. ADDRESS (City, State, and ZIP Code) Hanscom AFB MA 01731-5000		
8a. NAME OF FUNDING / SPONSORING ORGANIZATION Rome Air Development Center		8b OFFICE SYMBOL (if applicable) ESO	9 PROCUREMENT INSTRUMENT IDENTIFICATION NUMBER F19628-84-C-0015		
8c. ADDRESS (City, State, and ZIP Code) Hanscom AFB MA 01731-5000			10 SOURCE OF FUNDING NUMBERS		
			PROGRAM ELEMENT NO 62702F	PROJECT NO 4600	TASK NO 19
11 TITLE (Include Security Classification) SUPERLUMINESCENT LED STUDY					
12. PERSONAL AUTHOR(S) Robert Olshansky					
13a. TYPE OF REPORT Final		13b. TIME COVERED FROM Jun 84 to Dec 85		14. DATE OF REPORT (Year, Month, Day) November 1986	15 PAGE COUNT 26
16 SUPPLEMENTARY NOTATION N/A					
17 COSATI CODES			18 SUBJECT TERMS (Continue on reverse if necessary and identify by block number) Laser source spectral width LED anti-reflection coating superradiant		
FIELD	GROUP	SUB-GROUP			
20	06				
20	12				
19 ABSTRACT (Continue on reverse if necessary and identify by block number) This is the final report for a contract to develop superluminescent LEDs (SLEDs) for use with graded-index multimode fibers. The basic technical objective is to develop a SLED which can couple at least 500 μ W of power into a standard 0.20 NA 50- μ m core graded-index fiber at a drive current not exceeding 200 mA. The program objectives have been met and exceeded. Three devices mounted in a standard package with thermo-electric cooler (TEC) and graded-index fiber pigtail have been shipped to the customer.					
20 DISTRIBUTION / AVAILABILITY OF ABSTRACT <input type="checkbox"/> UNCLASSIFIED/UNLIMITED <input checked="" type="checkbox"/> SAME AS RPT <input type="checkbox"/> DTIC USERS			21 ABSTRACT SECURITY CLASSIFICATION UNCLASSIFIED		
22a. NAME OF RESPONSIBLE INDIVIDUAL Joseph P. Lorenzo			22b TELEPHONE (Include Area Code) (617) 861-3598		22c OFFICE SYMBOL RADC (ESO)

DD FORM 1473, 84 MAR

83 APR edition may be used until exhausted.
All other editions are obsolete

SECURITY CLASSIFICATION OF THIS PAGE

UNCLASSIFIED

I. Introduction

This is the final report for a contract to develop superluminescent LEDs (SLEDs) for use with graded-index multimode fibers. The basic technical objective is to develop a SLED which can couple at least 500 μ W of power into a standard 0.20 NA 50- μ m core graded-index fiber at a drive current not exceeding 200 mA. The program objectives have been met and exceeded. Three devices mounted in a standard package with thermo-electric cooler (TEC) and graded-index fiber pigtail have been shipped to the customer.

II. Antireflection Facet Coating

The principal new task for this project was to develop a technique for depositing high quality antireflection dielectric coating on the facet of vapor-phase regrown buried heterostructure (VPR-BH) lasers. Initial efforts concentrated on the plasma-assisted chemical vapor deposition of silicon nitride films on test wafers and subsequently on mounted devices. Low reflectivity silicon nitride coatings could be achieved on individual devices by adjusting the coating thickness with chemical etchants after deposition. However, the absence of a thickness monitor in the deposition system and the poor spatial uniformity of films deposited on large area wafers represented a significant limitation of this approach.

<input checked="" type="checkbox"/>
<input type="checkbox"/>
<input type="checkbox"/>



Availability Codes	
Dist	Available/ or Special
A-1	

Subsequent work was based on the use of electron-beam evaporated zirconium dioxide films having a refractive index of 1.80 to 1.95. Initial runs were made using large area silicon wafers to establish the proper deposition conditions and optimal film thickness. The development was completed by depositing films on the facets of mounted devices.

The quality of the coating deposited on a device facet was evaluated by monitoring the power-current output from front and rear facets of the device, both before and after deposition of the coating. A typical result is shown in Figure 1. The device had a cavity length of 200 μm and cavity width of 14 μm . The initial threshold current was 70 mA and the differential quantum efficiencies (DQE) from the front and rear facets were equal. After deposition of the zirconium dioxide film, the threshold current of the device exceeded 200 mA, and the ratio, x , of the DQE from front and rear facets was 12. From the expression

$$x = \frac{\eta_{D_f}}{\eta_{D_r}} = \sqrt{\frac{R_r}{R_f}} \left(\frac{1 - R_f}{1 - R_r} \right) \quad (1)$$

where R_r = rear facet reflectivity = .3

where R_f = front facet reflectivity,

it can be determined that the corresponding front facet reflectivity of the coated device is 0.4%. This represents a typical value that has been achieved, with best efforts yielding reflectivities of 0.1%. These values for the front facet reflectivity are adequate for the present application.

III. Wafer Processing

The SLEDs have been made by forming VPR-BH devices by the same basic process used to make lasers. The mask set used for processing produces devices with active layer widths of 14, 18, 22, and 26 μm . Standard double heterostructure laser wafers were grown using liquid phase epitaxy with InGaAsP active layers 0.2 μm thick. Double channels were etched in the wafer surface to form mesas with tops 14 to 26 μm wide. A preferential etchant was used to etch away the outer 1 to 2 μm of active layer, and vapor phase regrowth was used to fill in the etched groove. The resulting active layer completely buried in InP can be seen in the SEM photograph of Figure 2. The wafer was subsequently processed by standard methods to make a Zn/Au alloyed p-contact to the mesa top and a Au/Ge/In contact to the n-InP substrate side.

The first wafer processed for this study produced no lasers for reasons which could not be determined. The next two wafers produced excellent quality wide-stripe VPR-BH lasers with average threshold current densities of 2.0 to 2.5 kA/cm^2 . These are equivalent to broad area thresholds typically achieved for 200- μm cavity length devices. All subsequent SLEDs for testing or packaging have been taken from these two wafers.

IV. Optical Characteristics

Table I contains typical results obtained from SLEDs made from wafer 522. At 200 mA drive current, the total output power varied between 2.4 and 3.5 mW, and the temperature sensitivity of the output varied from 2.0 to 3.4%/°C.

The front facet reflectivity, inferred from the ratio of front and rear facet DQEs, varied between 0.2 and 2%. From the standpoint of temperature sensitivity, the devices with wider active layers have smaller temperature coefficients. This is the expected result since the wider devices operate lower down on the output power curve where the temperature sensitivity of the gain coefficient is less important. As discussed in the following section, the narrow devices afford higher power coupling efficiency and thus appear to have the overall best performance characteristics.

Figure 3 shows the cw output characteristics from a typical 14- μm SLED operated at 20°C. The power-current characteristic is only slightly superlinear, and a total output power of 2.4 mW is achieved at 200 mA. The temperature dependence of the output power is indicated in the inset of Figure 3.

Figure 4 shows the full width at half-maximum (FWHM) of the output spectrum of an 18- μm wide SLED as a function of drive current. The spectral width decreases from 62 nm at 50 mA to 32 nm at 200 mA.

V. Fiber-Coupled Power

A study has been carried out of the fiber-coupling efficiency of these SLEDs as a function of stripe width and drive current. The fiber is 0.20 NA 50- μm core graded-index fiber with a hemispherical epoxy lens formed on the fiber end. A typical example of the fiber-coupled power-current curve is shown in Figure 3. At 200 mA, 700 μW of fiber-coupled power is achieved with a coupling efficiency of 29%.

Figure 5 contains data on the fiber-coupled power achieved at 100 and 200 mA as a function of the active layer width of the SLEDs. At 200 mA, the

fiber-coupled power decreases by almost a factor of two as the active width increases from 14 to 26 μm . This corresponds to a drop in coupling efficiency from 29 to 16%.

Figure 6 shows the temperature dependence of the output power as a function of active layer width. At 200 mA drive current, the temperature dependence decreases from 2.7 to 2.0%/°C as the width varies from 14 to 26 μm .

In spite of the reduced temperature sensitivity and the lower operating current density of the devices with wider active layers, the predominate design consideration for the present application is high fiber-coupled power. On this basis, Figure 5 makes it clear that the narrower devices should be selected. Accordingly, 14- μm wide VPR-BH SLEDs have been chosen as the devices to be used for final packaging.

VI. Packaging

A number of 14- μm wide devices have been mounted in the standard dual-in-line package used for laser sources. Devices are mounted on a Au-plated copper submount which is in turn mounted on a TEC. The graded-index fiber with a hemispherical lens is epoxied in place and the lid is welded on in a dry nitrogen atmosphere. The temperature of the copper submount is monitored with a thermistor and the temperature can be maintained at a designated set point over an ambient temperature range of -30° to 80°C.

A number of 14 μm wide SLED chips were bonded to gold-plated copper submounts and given a 50°C-200 hour burn-in at an operating current of 70 mA in order to eliminate devices with high initial degradation rates. After initial burn-in ZrO_2 anti-reflection (AR) coatings were applied to the front facets of

the mounted devices. The AR coated SLEDs exhibited pulsed threshold currents of 130 to 150 mA, as compared to 70 mA for uncoated devices. The increase in threshold current implies that the front facet reflectivity of these devices is approximately 2%.

AR coated SLEDs were mounted in GTE Laboratories DIP-TEC-PACs and coupled to standard 0.2 NA 50 μm core multimode fiber. Figure 7 displays a representative power-current characteristic of a packaged fiber-coupled SLED. A cw output power of 500 μW , satisfying the contract goal, is obtained at a drive current of 120 mA. Figure 8 shows the variation in spectral width and peak emission wavelength as a function of drive current. At 120 mA the spectral width is 45 nm centered at a wavelength of 1.275 μm .

The temperature coefficient of the fiber-coupled power is plotted in Figure 9. At 120 mA the temperature coefficient is 6%/°C. The temperature coefficient of the fiber coupled power is a factor of three higher than the temperature coefficient of the total output power previously reported for un-packaged SLEDs. The increased temperature coefficient of the fiber-coupled SLEDs is of no practical importance since the built-in thermoelectric cooler will hold the device temperature at 20° C over an ambient temperature range of -30° C to +80° C. The higher temperature coefficient results in part from the fact that stimulated emission couples more efficiently into the fiber than spontaneous emission.

The packaged SLEDs described above have been burned in for 200 hours at 20° C with no significant change in power-current characteristics. Three of these packaged devices have been shipped to the customer.

VII. Conclusions

The vapor phase regrowth process has been demonstrated to be a successful, reproducible method for producing wide cavity double heterostructure chips suitable for making superluminescent LEDs. The required antireflection facet coatings have been produced by use of electron-beam evaporated zirconium oxide films and facet reflectivities of 1-2 % have been reproducibly demonstrated.

Fiber coupled powers well in excess of the 500 μW required by the contract have been achieved at drive currents of 200 mA. Three devices have been supplied to the customer mounted in the GTE DIP-TEC-PAC coupled to 0.20 NA 50 μm core graded-index fiber. The packaged devices satisfied the contract goal of 500 μW at a drive current of 120 mA.

Figure Captions

- Figure 1. Power-current characteristics for a 14- μm SLED before and after application of the ZrO_2 facet coating. The ratio of front-to-rear slope efficiency provides a measure of the facet reflectivity.
- Figure 2. An SEM micrograph showing the cross section of a VPR-BH SLED with an 18- μm wide active region.
- Figure 3. Power-current characteristics for a 14- μm SLED showing the total output power and the power coupled to a 0.20-NA, 50- μm core graded-index fiber with a hemispherical lens.
- Figure 4. Full width at half-maximum of the output spectrum as a function of drive current.
- Figure 5. (a) Fiber-coupled power at 100 and 200 mA.
(b) Coupling efficiency.
(c) Total output power as a function of active layer width.
- Figure 6. The temperature dependence and operating current density is shown as a function of active layer width.
- Figure 7. Power-current curve of fiber-coupled SLED.
- Figure 8. Spectral width and peak wavelength of fiber-coupled SLED emission.
- Figure 9. Temperature coefficient of fiber-coupled SLED emission.

Table Captions

Table I. Stripe width, output power, temperature coefficient and facet reflectivity for a number of SLEDs from wafer #522.

FACET REFLECTIVITY IS FOUND FROM COMPARISON OF FRONT AND REAR FACET P-I CURVES

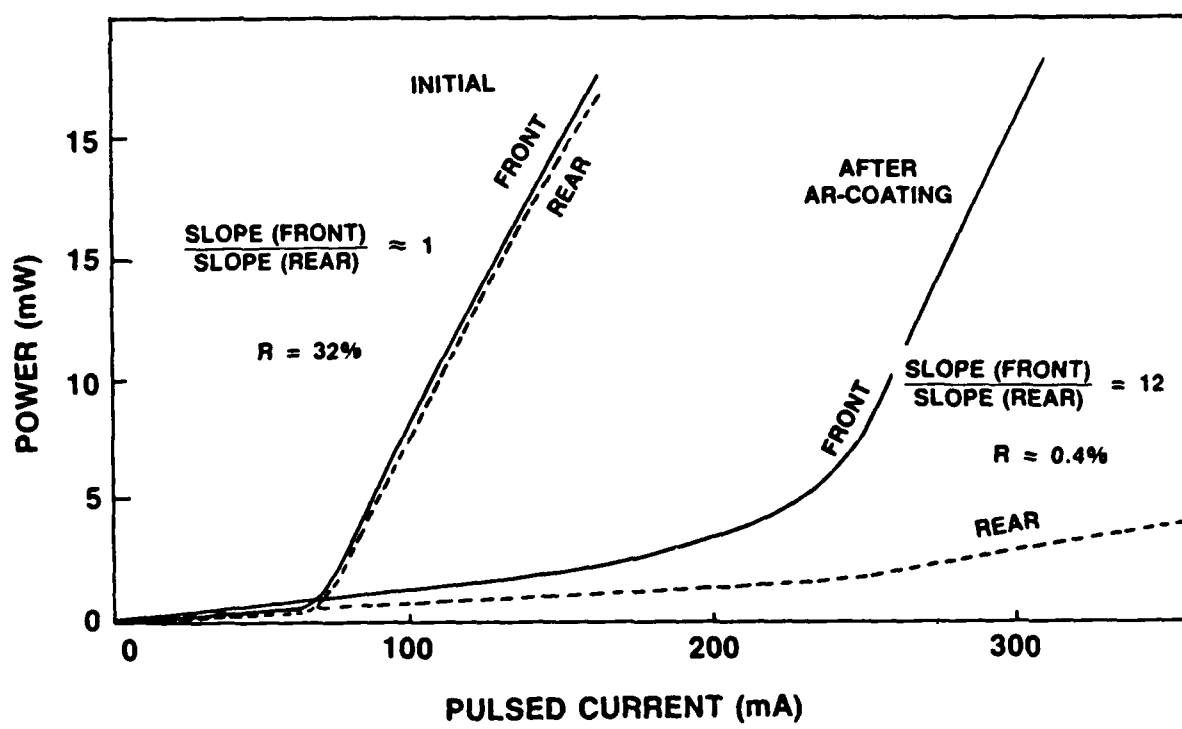


Figure 1

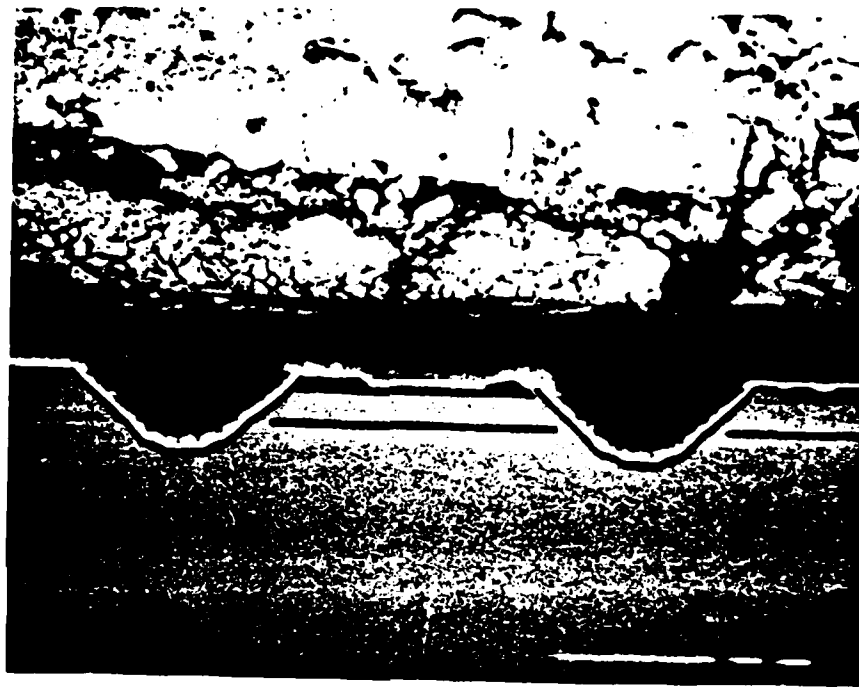


Figure 2

OUTPUT POWER FROM 14 μm ELED

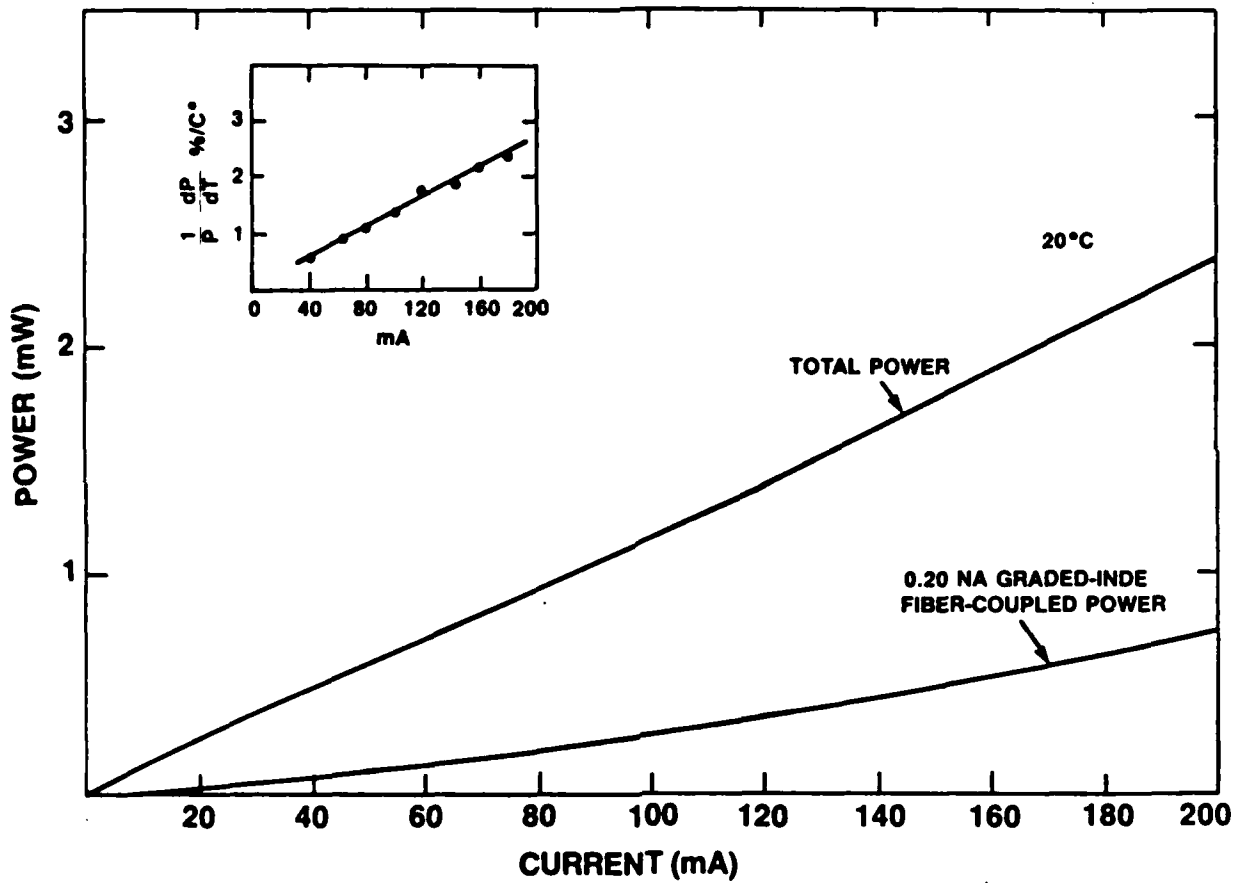
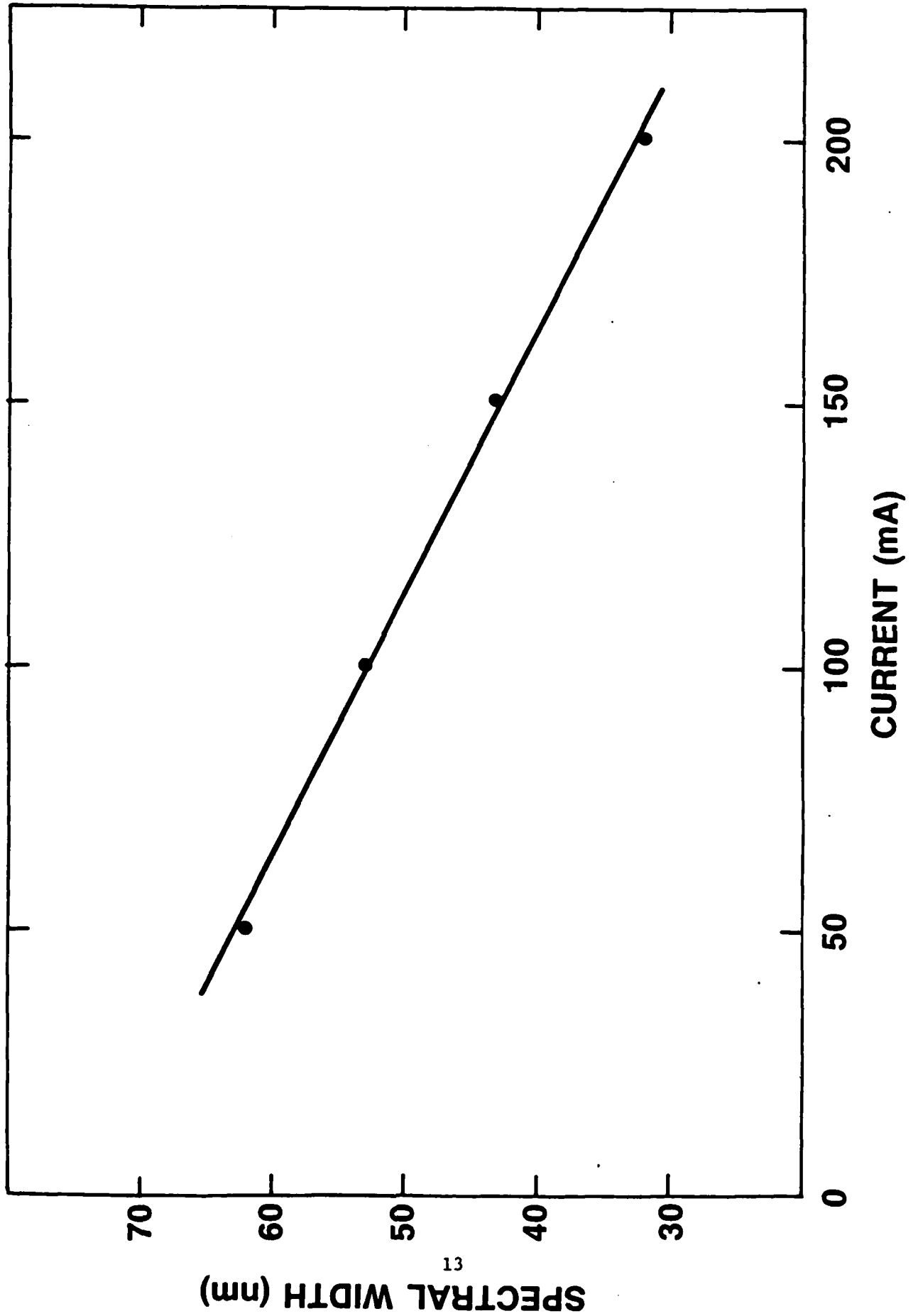


Figure 3

Figure 4

18 μm SLED



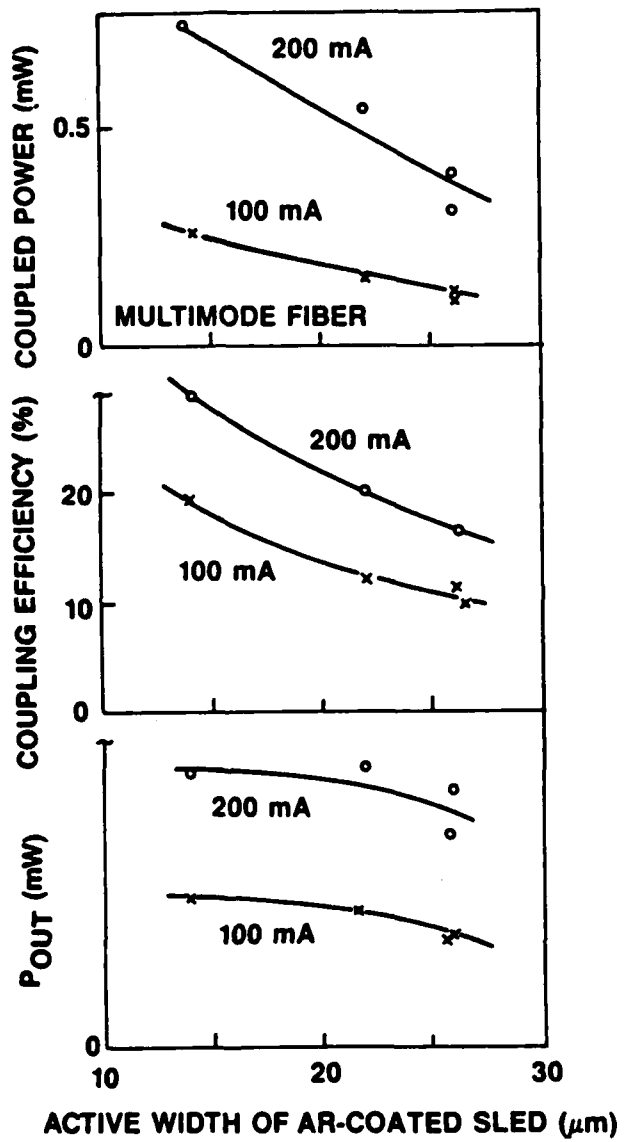


Figure 5

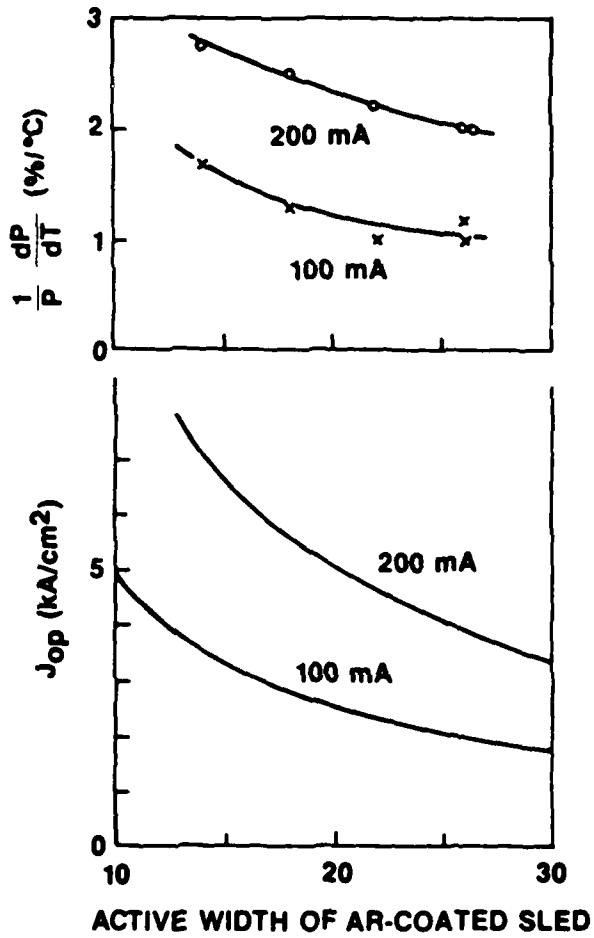


Figure 6

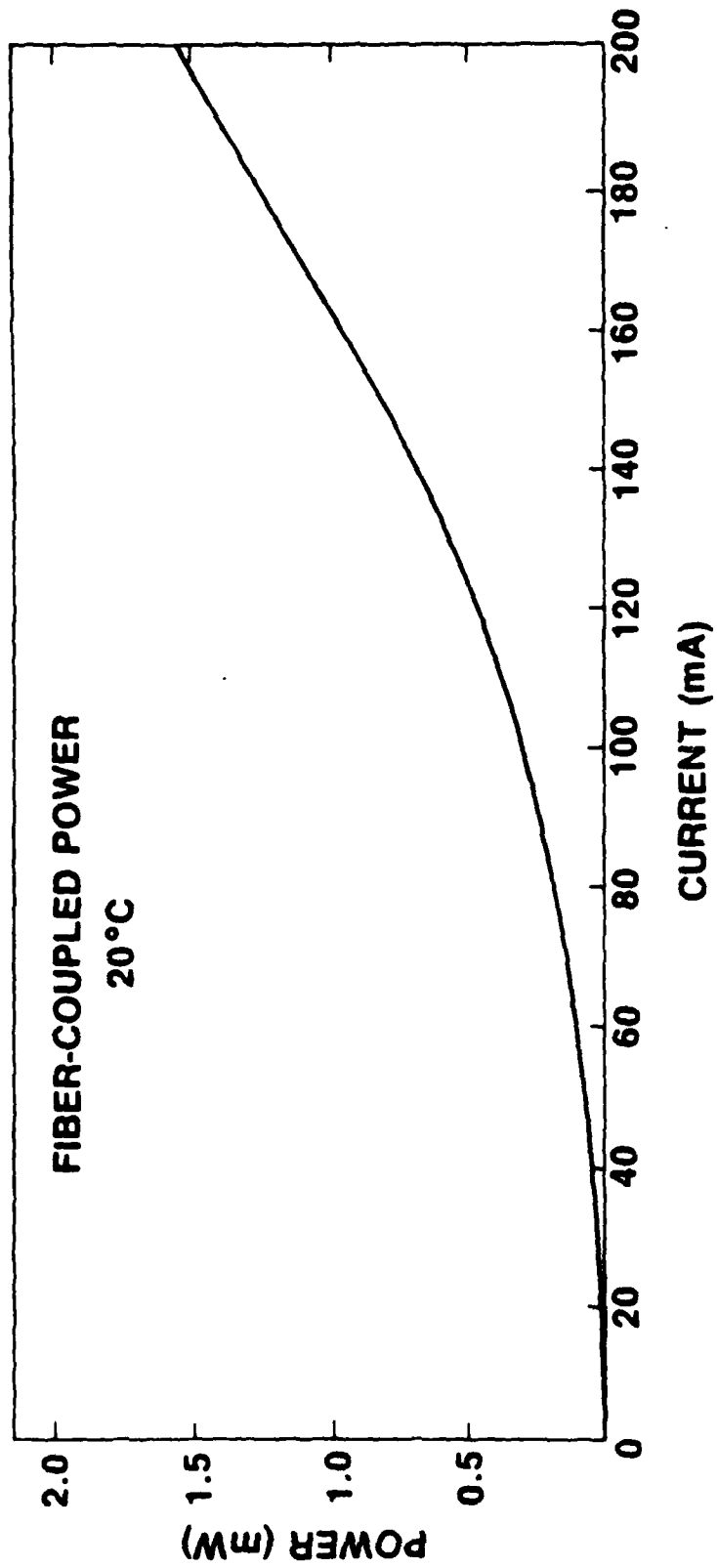


Figure 7

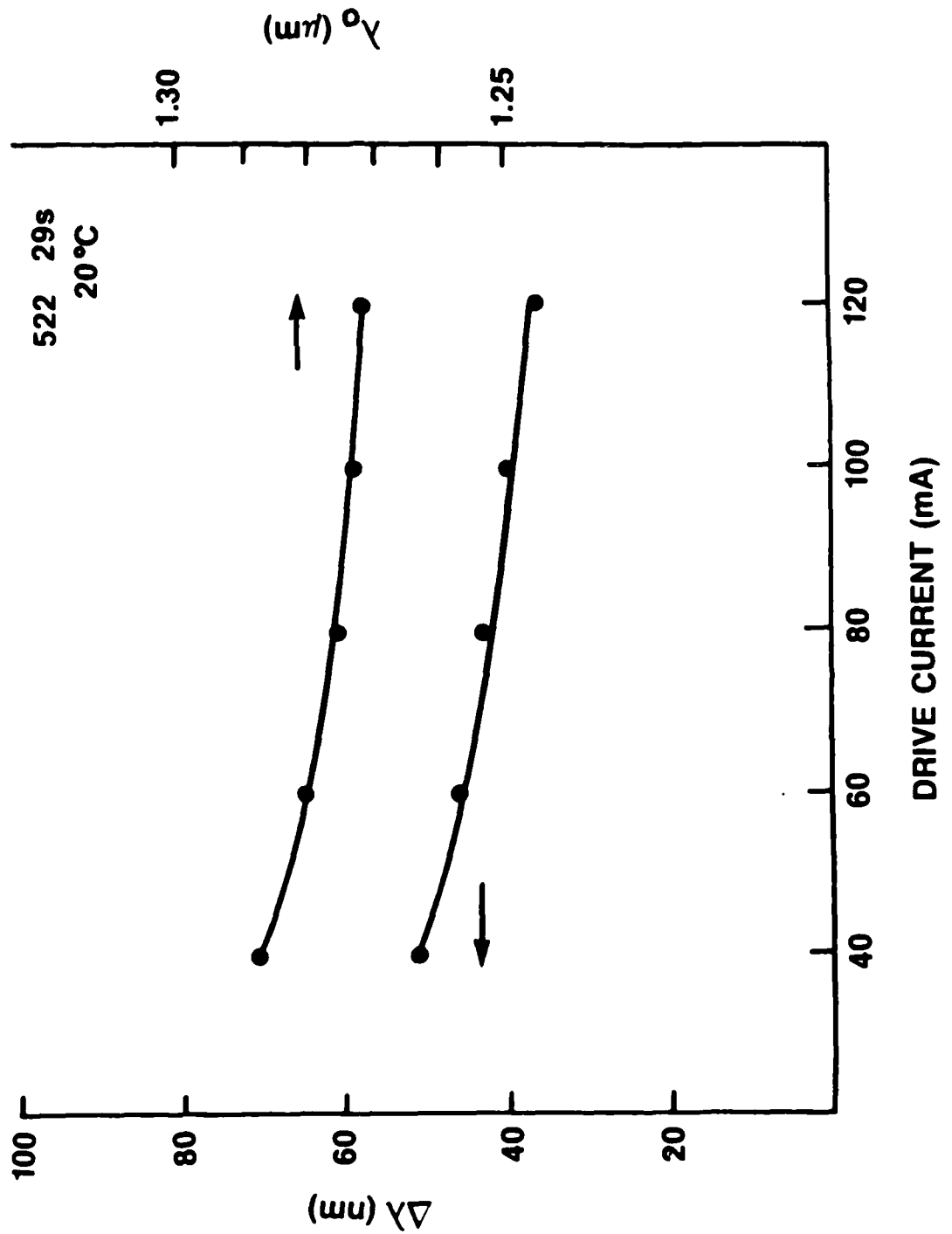


Figure 8

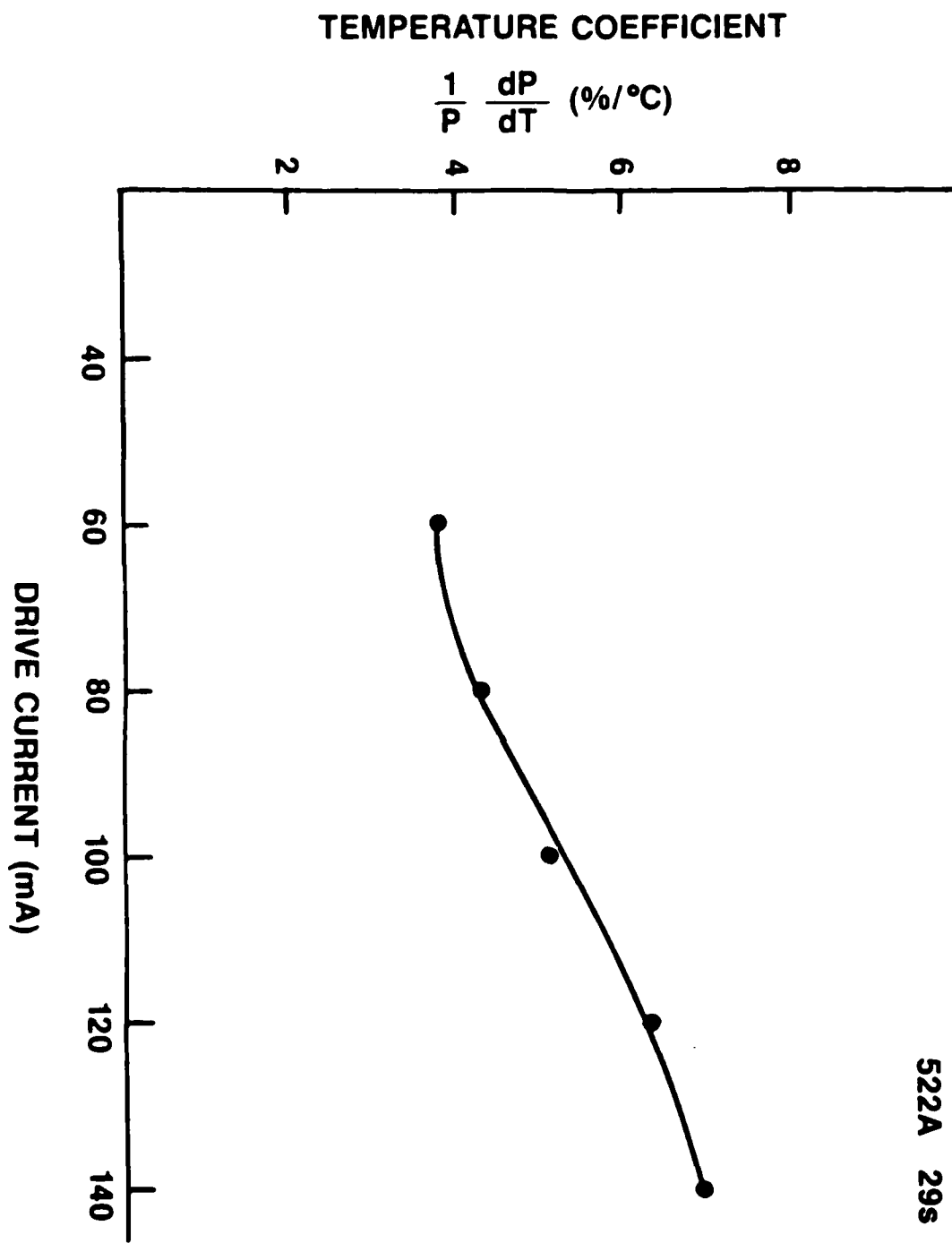
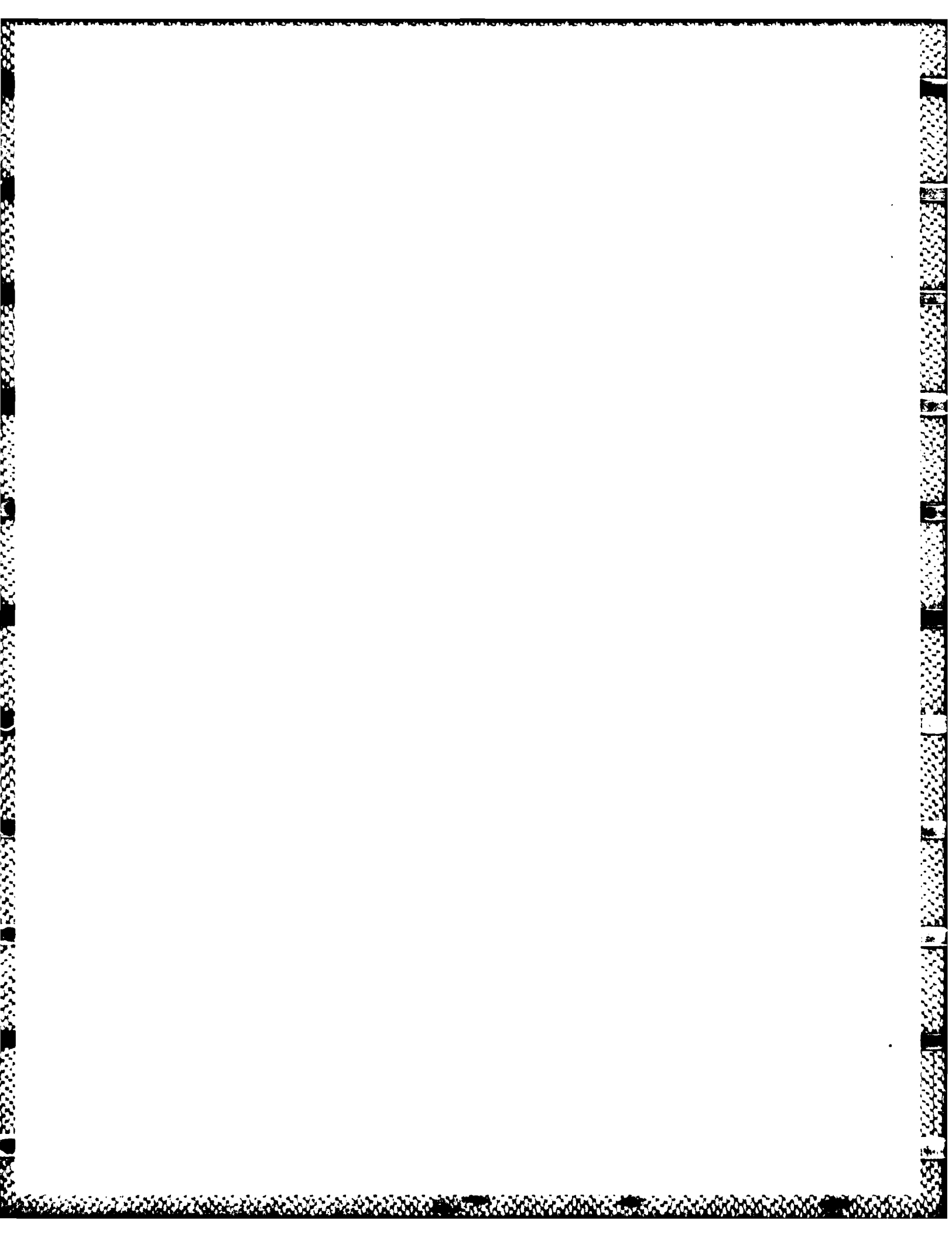
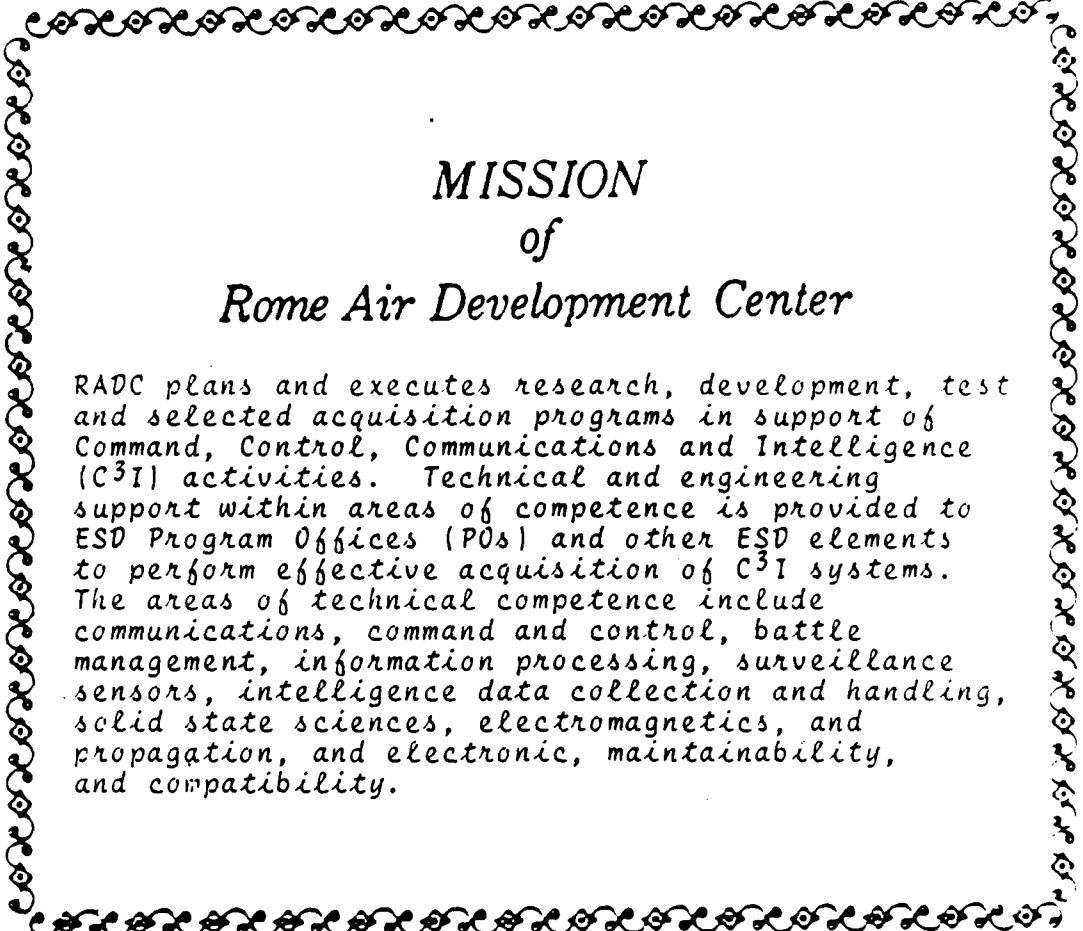


Figure 9

TABLE 1

DEVICE	STRIPE WIDTH (μm)	P(200 mA) (mW)	$\frac{1}{P} \frac{dP}{dT}$ (% $^{\circ}\text{C}$)	R(%)
522-14-6	14	3.5	3.4	0.3
522-14-8	14	2.4	2.4	0.2
522-18-1	18	2.4	2.7	1.
522-22-3	22	2.4	2.1	0.6
522-22-5	22	3.0	---	2.0
522-26-2	26	2.4	1.9	0.3
522-26-4	26	2.6	2.0	0.7
522-26-1	26	2.8	---	0.3





MISSION
of
Rome Air Development Center

RADC plans and executes research, development, test and selected acquisition programs in support of Command, Control, Communications and Intelligence (C³I) activities. Technical and engineering support within areas of competence is provided to ESD Program Offices (POs) and other ESD elements to perform effective acquisition of C³I systems. The areas of technical competence include communications, command and control, battle management, information processing, surveillance sensors, intelligence data collection and handling, solid state sciences, electromagnetics, and propagation, and electronic, maintainability, and compatibility.

END

5-87

DTIC